Supporting Information

Lateral heterostructures of monolayer group-IV monochalcogenides: band alignment and electronic properties

Kai Cheng [a], Yu Guo [a], Nannan Han [a], Yan Su [a*], Junfeng Zhang [b], Jijun Zhao [a,c*]

[a] *Key Laboratory of Materials Modification by Laser, Ion and Electron Beams (Dalian University of Technology), Ministry of Education, Dalian 116024, China*

[b] *School of physics and information Engineering, Shanxi Normal University, Linfen 041000, China*

[c] *Beijing Computational Science Research Center, Beijing 100094, China*

* Corresponding authors. Y. Su (e-mail: su.yan@dlut.edu.cn) or J. Zhao (e-mail: zhaojj@dlut.edu.cn).

Table S1 Lattice mismatches of four monolayer heterostructures along armchair and zigzag directions.

	GeS/GeSe	SnS/GeSe	SnSe/GeS	GeS/SnS
armchair	3.18%	< 0.001%	0.2%	3.18%
zigzag	7.77%	2.45%	13.82%	10.02%

Table S2 Conduction band offset (CBO) and valence band offset (VBO) of monolayer heterostructures from both PBE and HSE06 calculations. CBO is the difference of χ between two isolated monolayer group-IV monochalcogenide, while VBO is the difference of *I*. All parameters in this table are in the unit of eV.

	GeS/GeSe		SnS/GeSe		SnSe/GeS		GeS/SnS	
	VBO	CBO	VBO	CBO	VBO	CBO	VBO	CBO
HSE06	–0.43	0.19	–0.09	0.29	–0.69	0.16	–0.34	–0.10
PBE	–0.43	0.08	–0.05	0.26	–0.69	0.07	–0.38	–0.19

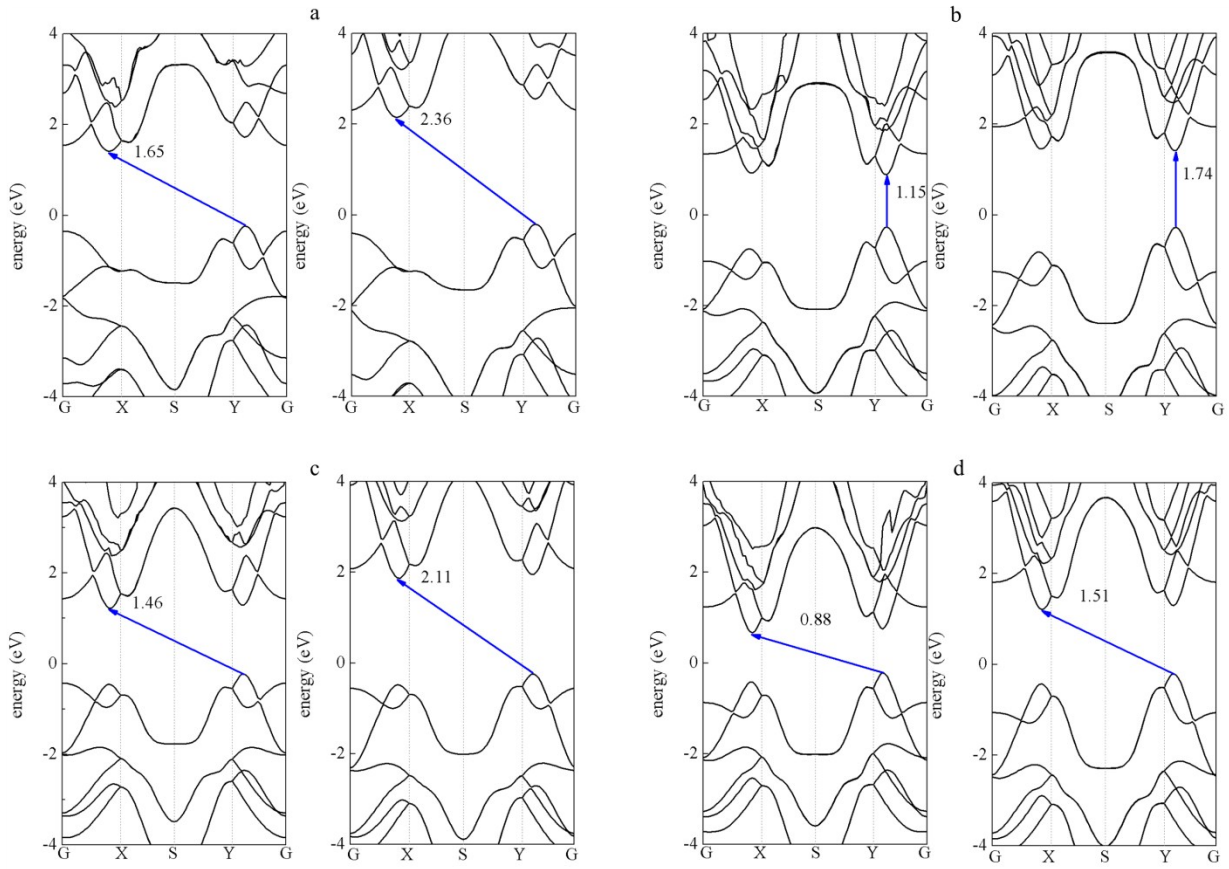

Fig. S1 Calculated band structures of individual (a) GeS, (b) GeSe, (c) SnS and (d) SnSe monolayers using both PBE (left) and HSE06 (right) methods.

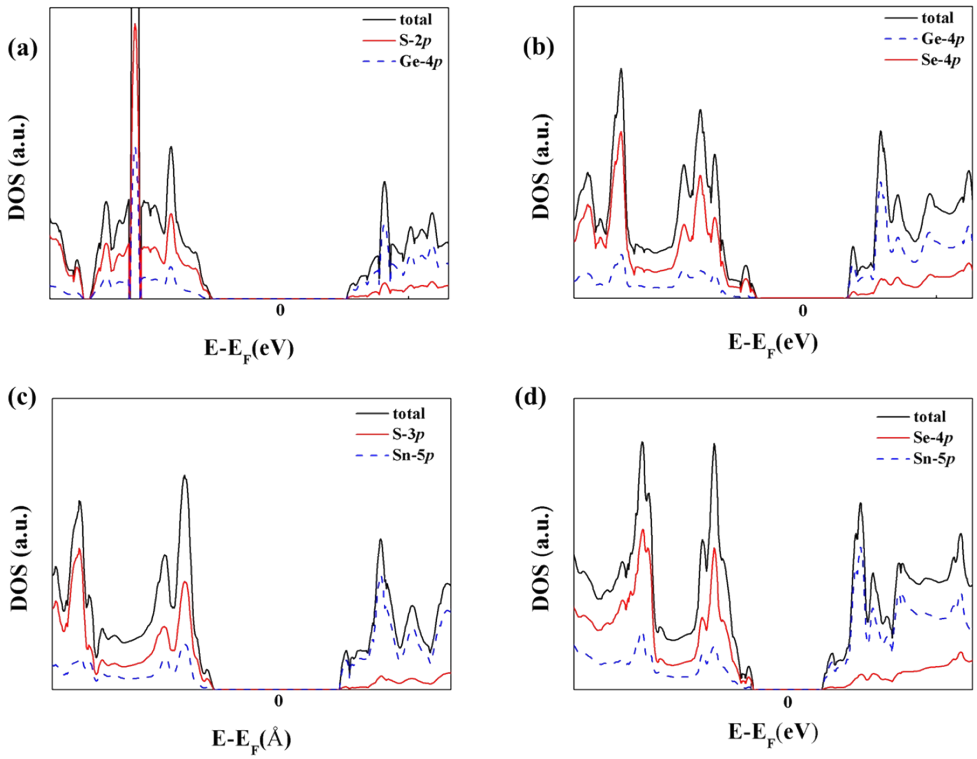

Fig. S2 Total DOS and partial DOS of individual (a) GeS, (b) GeSe, (c) SnS and (d) SnSe monolayers. The black solid lines, the red solid lines and blue dashed lines represent the total DOS, the *p* orbitals of S/Se and Ge/Sn, respectively.

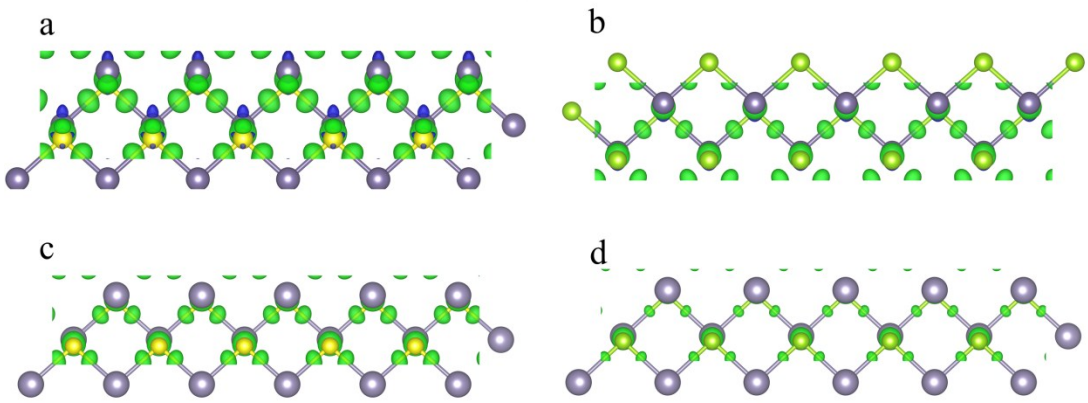

Fig. S3 The charge density difference of individual (a) GeS, (b) GeSe, (c) SnS and (d) SnSe monolayers with inclusion of five unit cells. The green and blue areas represent electron accumulation and depletion, respectively (isosurface value = 0.007 e per $Å^3$). One can see that GeS and SnS sheets exhibit stronger covalent bonding.

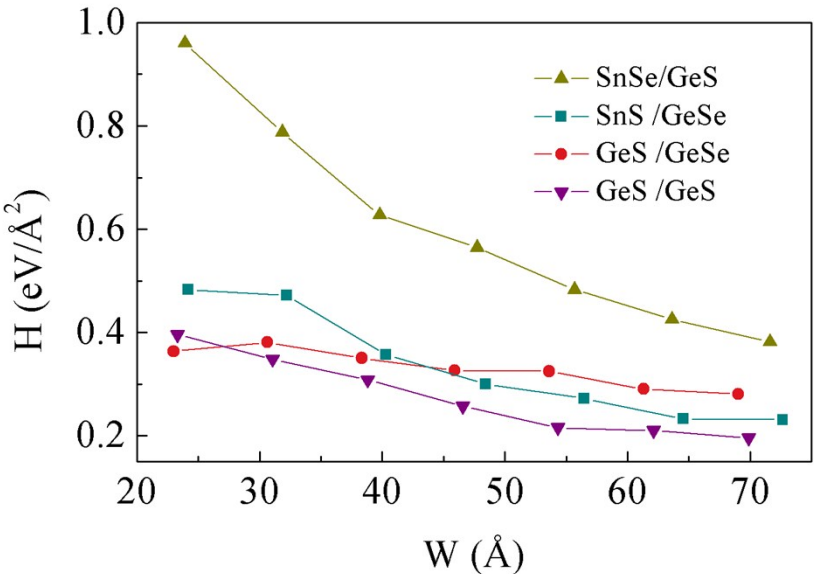

Fig. S4 Heat of formation (H_F) for monolayer GeS/GeSe (red), GeS/SnS (purse), SnSe/GeS (green), and SnS/GeSe (blue) heterostructures with different supercell widths (W) in the *x* direction from PBE calculations. The heat of formation have no obvious change with the increase of supercell width W from 20 to 75 nm (the largest change is 0.5 eV/Å^2).

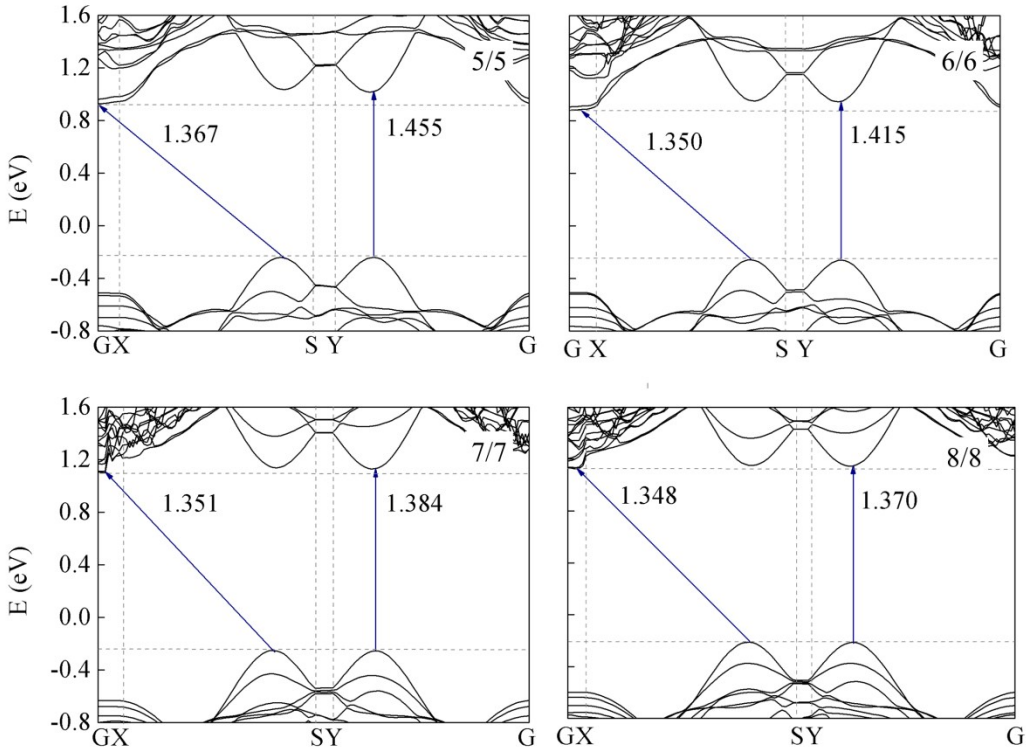

Fig. S5 Band structures of monolayer GeS/GeSe with different widths. Here, index *n*/*n* means that there are *n* unit cells on the left domain and *n* unit cells on the right one.

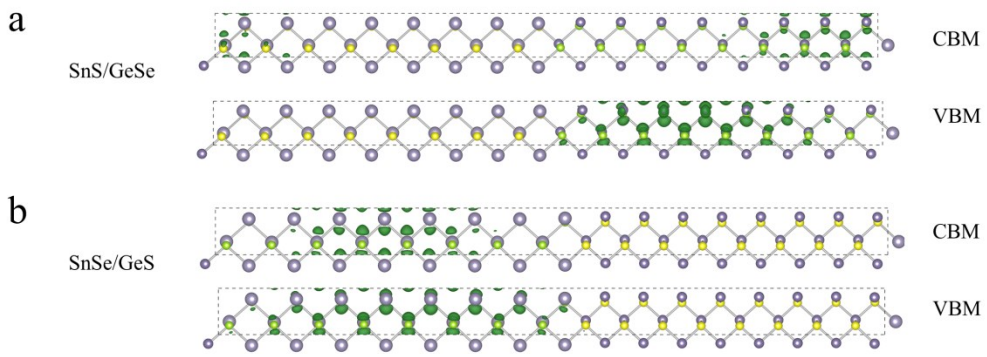

Fig. S6 The partial charge distributions corresponding to the VBM and CBM for monolayer (a) SnS/GeSe and (b) SnSe/GeS heterostructures.

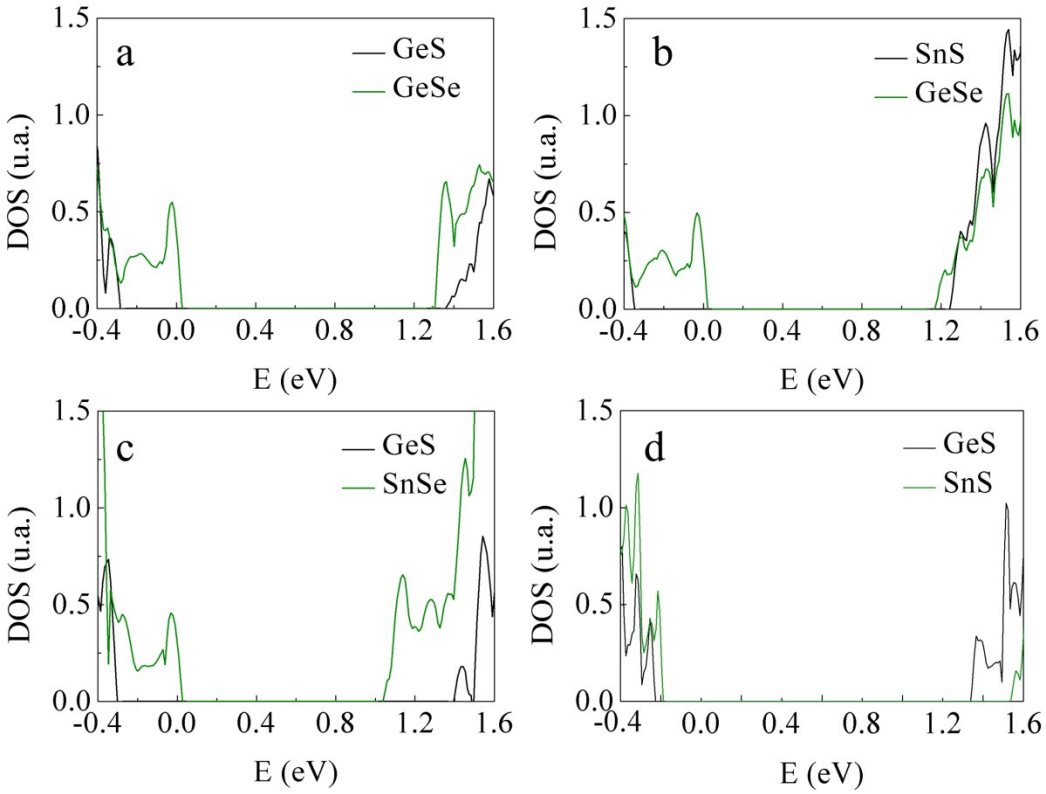

Fig. S7 LDOS of monolayer (a) GeS/GeSe, (b) SnS/GeSe, (c) SnSe/GeS and (d) GeS/SnS. For convenient, the 9/9 supercells are used for all calculation of LDOS, and the LDOS comes from the center unit, i.e. fifth unit in each domain.

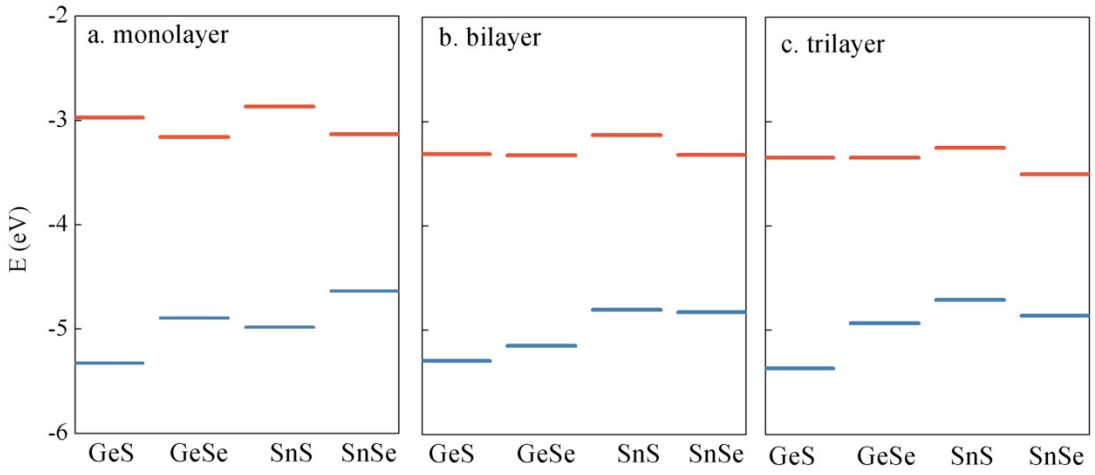

Fig. S8 Band-edge positions of isolated (a) monolayer, (b) bilayer and (c) trilayer group-IV monochalcogenides relative to the vacuum level (zero energy) calculated using the HSE06 functional. In each plot, the orange is for conduction band minimum (CBM) and the blue (lower) is for valence band maximum (VBM).

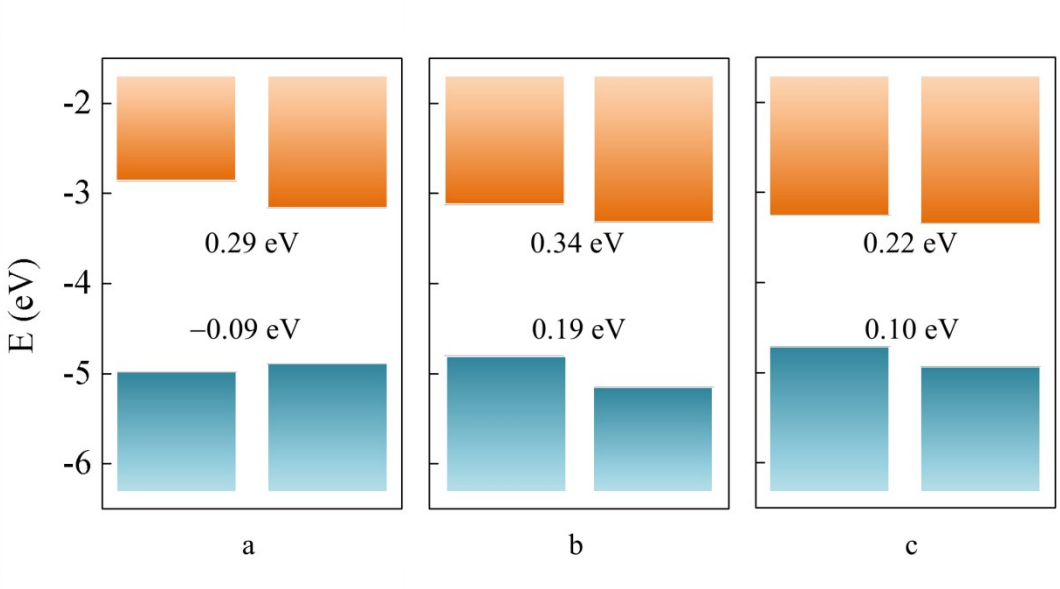

Fig. S9 Band alignments of (a) monolayer (b) bilayer and (c) trilayer SnS/GeSe heterostructures at Anderson limit calculated using the HSE06 functional. In each plot, the orange (upper) is for conduction band and the blue (lower) is for valence band; the upper number is conduction band offset (CBO), and the lower number is valence band offset (VBO). The vacuum level is set to zero energy.